

Stationary transport above the critical velocity in a one-dimensional superflow past an obstacle

J. HUYNH¹, F. HÉBERT¹, P.-É. LARRÉ¹ and M. ALBERT^{1,2(a)} 

¹ *Université Côte d'Azur, CNRS, Institut de Physique de Nice - 06200 Nice, France*

² *Institut Universitaire de France (IUF)*

received 13 June 2023; accepted in final form 17 August 2023

published online 29 August 2023

Abstract – We consider in this work the different possible stationary flows of a one-dimensional quantum fluid in the mean-field regime. We focus on the supersonic regime where a transition from a time-dependent flow to a stationary diffractive flow occurs at a given critical velocity. We give nonperturbative results for this critical velocity in the presence of a localised obstacle of arbitrary size and strength. In addition, we discuss the existence of superfluid-like solution in the supersonic regime due to resonant transport and provide a complete map of the different regimes of stationary transport of a quantum fluid.

Copyright © 2023 EPLA

Introduction. – One important property of superfluids is their ability to move without dissipation below a certain critical velocity v_c [1]. A phase transition occurs at v_c and the superfluid behaves as a normal dissipative fluid for velocities larger than v_c . First observed in liquid helium [2,3], superfluidity was later shown to be more generic and was observed in various quantum fluids [4–7]. Soon after its discovery, the critical velocity was theorised by Landau [8,9] who proposed a very elegant and general criterion which states that $v_c = \min_{\mathbf{p}} \varepsilon(\mathbf{p})/p$, where $\varepsilon(\mathbf{p})$ is the spectrum of elementary excitations with momentum \mathbf{p} . However, this prediction usually overestimates the actual critical velocity and was verified experimentally only under very specific configurations as, for instance, by moving a single ion in liquid helium [10]. The reason is that Landau's argument is perturbative and therefore does not take properly into account the nonlinear nature of the problem of interaction between quantum fluids and external potentials. Important progresses arose with the introduction of a simpler model to describe the flow of a quantum fluid: The nonlinear Schrödinger (NLS) equation or Gross-Pitaevskii (GP) equation [11–13]. In particular, nonperturbative results were derived for the first time by Frisch and collaborators in two dimensions in the presence of an impenetrable cylinder [14] followed by a series of works for various obstacles (see ref. [15] for a review). Although this model is not satisfactory for the description of dense systems such as liquid helium, it is very accurate

for weakly interacting superfluids such as Bose-Einstein condensates [16] or quantum fluids of light [17].

However, the transport properties of quantum fluids described by a NLS equation are not restricted to superfluidity and display a rich phenomenology [18–21] which is summarised in fig. 1, for a one-dimensional system. In the presence of a localised obstacle, three different regimes of transport exist depending on its strength and relative velocity with the fluid. Below the actual superfluid critical velocity v_c , the flow is stationary and only locally perturbed in the vicinity of the obstacle, as illustrated in panel (a) of fig. 1. Above this threshold, which strongly depends on the obstacle, the flow can no longer be stationary due to the continuous emission of linear and nonlinear excitations (fig. 1(b)) which leads to a slowdown of the superfluid motion and possibly to wave and quantum turbulence [22,23]. At larger velocities, a second critical velocity, often referred to as the supersonic separatrix [18,24,25], separates the latter regime from another regime of stationary transport. We will denote this second critical velocity v_s . The high-velocity stationary regime observed for velocities larger than v_s is reminiscent of the linear Schrödinger equation since the kinetic energy becomes much larger than the interaction energy in the fluid. In that case, the flow is partly backscattered by the obstacle and generally experiences friction. The incoming and reflected flows interfere and create a standing wave with a density modulation ahead of the obstacle (fig. 1(c)). Yet some configurations exist in which dissipation does not occur, even in the nonsuperfluid phase, due to resonant transport [26–28]. For specific obstacle

^(a)E-mail: mathias.albert@univ-cotedazur.fr (corresponding author)

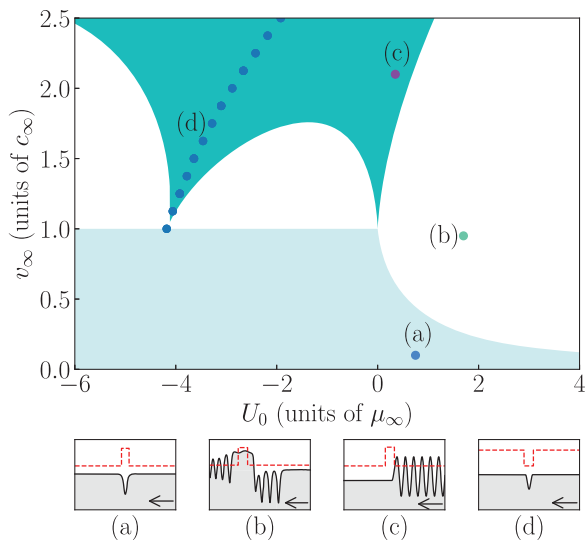


Fig. 1: Typical phase diagram of the possible stationary flows in the presence of a localised obstacle, hereby a square potential, as a function of the fluid velocity v_∞ and the strength of the obstacle U_0 . The different regimes range from a superfluid (light blue) to a normal stationary regime (dark blue), the white phase in between corresponds to the nonstationary nonsuperfluid regime. The dotted curve corresponds to a resonant state where the supersonic solution mimics the superfluid ones. Generic space-dependent density profiles $n(x)$ are given in panels (a), (b), (c) and (d), for the corresponding points in the phase diagram. This phase diagram was obtained for a cubic nonlinearity $g(n) = n$ and a square potential of width $\sigma = 1$ and amplitude U_0 . The units are detailed in the text.

parameters there might exist curves in the supersonic stationary phase where backscattering is suppressed and the fluid experiences no drag at all mimicking a superfluid solution (fig. 1(d)), a behaviour normally present below the superfluid critical velocity v_c , in the subsonic regime [29].

The aim of this letter is to determine, in a nonperturbative way, the supersonic separatrix —*i.e.*, the border between the nonstationary and the stationary nonsuperfluid regimes— for a generic quantum fluid flowing past a simplified localised obstacle in the one-dimensional mean-field regime. In addition, we study in detail the conditions to obtain superfluid-like solutions in the supersonic regime. Combined with previous results for the superfluid critical velocity [15], this work provides a complete map of the different possible regimes of stationary transport for a one-dimensional quantum fluid, above and below the sound velocity, for repulsive or attractive obstacles, and for different types of nonlinearities.

This paper is divided as follows: The model of the quantum fluid, based on a generalisation of the 1D nonlinear Schrödinger equation to any local self-interaction potential increasing with the fluid density, is first detailed. This general approach makes it possible to describe many superfluid systems ranging from ultracold atomic Bose and Fermi gases [16] to exciton-polariton condensates in semiconductor optical microcavities [6,17] and fluids of

light [7,21,30–34]. A thorough analytical study is then performed in the following sections in the limits of narrow or wide obstacles. Finally, we bridge the gap between these two limiting cases with a numerical study for a model obstacle and characterise analytically the perfect transmission lines.

Theoretical model. — We consider a one-dimensional quantum fluid flowing in the negative- x direction in the framework of the NLS equation. For the sake of clarity, we employ here the language of weakly interacting bosonic particles of mass m although the results derived in this paper are of wider interest. A quantum fluid dictionary is provided in the Supplementary Material [SupplementaryMaterial.pdf](#) (SM) for readers interested in other physical realisations of this model. The dynamics of the considered system is governed by a generalised nonlinear Schrödinger equation for the order parameter ψ ,

$$i\hbar\partial_t\psi = \left[-\frac{\hbar^2}{2m}\partial_{xx} + U(x) + g(|\psi|^2) \right] \psi. \quad (1)$$

The flow is here constrained by an obstacle described in eq. (1) by a potential $U(x) = U_0 f(|x|/\sigma)$ which attains its single positive maximum (negative minimum) U_0 at $x = 0$ and which is localised, *i.e.*, which vanishes as $|x| \gg \sigma$, with σ being its typical range. Throughout this work, we will exemplify our results with a repulsive (attractive) square potential $U(x) = U_0\Theta(\sigma/2 - |x|)$ but results with a Gaussian potential are given in the SM. The reason why we employ such a toy model is because it allows to obtain analytical results without loss of generality. In addition to the external potential, the fluid is also subjected to a self-interaction described by the local nonlinear term $g(|\psi|^2) = n\psi$, where the potential $g(n)$ is an increasing function of the density n . We consider two different kinds of nonlinearities. We mostly used the cubic nonlinearity of the standard NLS equation, where $g(n) = n$ in appropriately chosen units. This describes accurately dilute ultracold bosonic atoms [15]. We also considered a saturable nonlinearity of the form $g(n) = (1 + n_s)^2 n / [n_s(n + n_s)]$ which describes quantum fluids of light in rescaled units, where n is related to the light intensity and n_s to the saturation intensity in the nonlinear medium (see SM).

We now look for the existence of out-of-equilibrium stationary solutions of eq. (1) of the form $\psi(x,t) = \exp[-i\mu t/\hbar]A(x)\exp[i\varphi(x)]$, from which the density and the velocity fields are obtained from $n(x) = A(x)^2$, $v(x) = \hbar\varphi'(x)/m$ and μ is the chemical potential. This yields the following equation of motion for these fields:

$$\begin{aligned} n(x)v(x) &= \Phi, \\ -\frac{\hbar^2}{2m}A''(x) + \left[U(x) + g(n) + \frac{m\Phi^2}{2A(x)^4} \right] A(x) &= \mu A(x). \end{aligned} \quad (2)$$

The first of eqs. (2) is simply the current conservation while the second one expresses the space dependence of the

density and, therefore, the velocity through current conservation. These equations have to be complemented with boundary conditions. As explained in ref. [18], a regime of stationary flow exists for supersonic velocities, but in this case the radiation condition [35] requires that the wake is always located ahead of the obstacle, *i.e.*, upstream, with no long-range perturbation of the fluid on the downstream region, where the flow remains unperturbed. The solution has therefore to tend to a constant solution with density n_∞ and velocity v_∞ far away from the obstacle in the downstream region (in our case $x \rightarrow -\infty$) with $\Phi = n_\infty v_\infty$ and $\mu = \frac{1}{2} m v_\infty^2 + g(n_\infty)$. For comparison, a stationary superfluid solution satisfies the same condition in the upstream and downstream regions which is way more restrictive. Finally, two important scales emerge due to the nonlinearity $g(n)$, namely the sound velocity c_∞ and the healing length ξ_∞ . They are defined in the downstream region as $m c_\infty^2 = n_\infty g'(n_\infty) = \mu_\infty$ and $\xi_\infty = \hbar / m c_\infty$. In the rest of the paper we rescale all quantities in terms of n_∞ for densities, c_∞ for velocities, ξ_∞ for distances, and $m c_\infty^2$ for energies. This corresponds to the substitution $\hbar = m = 1$ and $\mu = g(1) + \frac{1}{2} v_\infty^2$ in eq. (2).

The main objective is now to search for the condition of existence for the solutions to eq. (2), which depends on the value of the injection velocity v_∞ . The last value under which there is no longer a solution to eq. (2) defines the equation of the supersonic separatrix. In the spirit of ref. [18], eq. (2) can be rephrased in terms of a Hamilton equation describing the dynamics of a fictitious classical particle of position $A(x)$ and momentum $p = A'(x)$ at time x . The corresponding Hamilton function reads [36]

$$\mathcal{H}(A, p) = \frac{p^2}{2} + W(A^2) - U(x)A^2 \quad (3)$$

with $W(A^2 = n) = \frac{v_\infty^2}{2} (n + \frac{1}{n}) + n g(1) - G(n)$, and the antiderivative $G(n) = \int dn g(n)$. Equations (2) are then derived from the canonical Hamilton equations $\dot{p} = -\partial_A \mathcal{H}$ and $\dot{A} = \partial_p \mathcal{H}$, where the dot stands for the total derivative with respect to the effective time x . In particular, in the absence of the external potential $U(x)$, this Hamiltonian is time-independent and the energy E_{cl} of the classical particle is conserved. The free solutions of the NLS equation can then be readily obtained from the possible trajectories of the classical particle in the potential $W(A^2 = n)$. The typical shape of this potential for $g(n) = n$ is depicted in fig. 2. For example, the equilibrium point referred to as n_∞ in fig. 2 corresponds to a constant-density supersonic solution ($v_\infty > c_\infty$) while small oscillations around this classical fixed point correspond to the superposition of an incoming plane wave and a small-amplitude reflected wave describing weak backscattering. Note that, in general, the nonlinearity of the NLS equation forbids such a separation of the upstream solution into a sum of independent incoming and reflected waves. However, if the backscattering is weak, the interaction between the incoming wave and the reflected wave is negligible. In general, this separation is

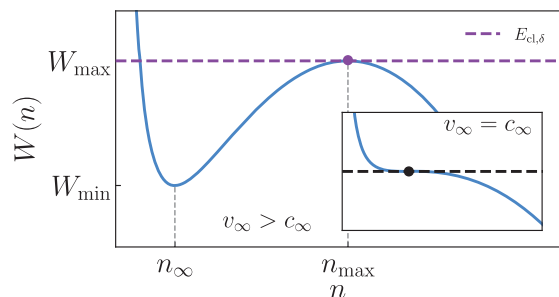


Fig. 2: Schematic behaviour of the fictitious potential $W(A^2 = n)$ for a cubic nonlinearity of the form $g(n) = n$ and $v_\infty > c_\infty$. The inset displays the special case $v_\infty = c_\infty$.

not possible and the free solutions are described by cnoidal waves [18]. In particular, solutions with E_{cl} slightly below W_{max} correspond to one or several gray solitons. In the presence of the scattering potential $U(x)$ the energy of the classical particle is no longer conserved and its dynamics may be nontrivial. The boundary condition in the downstream region (where $U(x) = 0$) imposes that the classical particles starts with $A(-\infty) = 1$ (n_∞ in fig. 2) and the forward integration has to satisfy that the final energy and the position A of the classical particle remain in the well of $W(n)$. This is the strategy we use to obtain the equation of the supersonic separatrix.

In the following we provide explicit analytical results for the supersonic separatrix in the limiting cases of weak, narrow and wide obstacles. We then focus on the case of the attractive obstacle of arbitrary width. Using numerical solutions, we identify resonant transport and solutions with perfect transmission similar to the ones of the superfluid regime. Our study reveals the existence of resonances for very specific sets of injection velocity and obstacle parameters as can be seen in fig. 1, which we characterise in the context of our simplified model, providing a better comprehension of the phenomenon.

Weak obstacle. – Before discussing nontrivial situations, it is instructive to revisit Landau’s criterion, which in our case reduces to the well-known result $v_c = c_\infty$, in terms of the classical mechanics analogy. The fictitious potential $W(n)$ must be typically of the shape shown in fig. 2, with $\lim_{n \rightarrow 0} W(n) = +\infty$ and $\lim_{n \rightarrow +\infty} W(n) = -\infty$. $W(n)$ has a local minimum W_{min} obtained at $n_\infty = 1$, and a local maximum W_{max} for $n_{max} > 1$. In the absence of any scattering potential, solutions with $n = n_\infty$ and $n = n_{max}$ correspond respectively to the supersonic and the subsonic superfluid solution. As v_∞ is tuned and approaches c_∞ these two solutions merge and the potential has a saddle point as shown in the inset of fig. 2. The two critical velocities v_c and v_s are therefore identical and equal to the speed of sound as shown in fig. 1 for $U_0 \rightarrow 0$. The presence of a weak obstacle will not modify the structure of this saddle-node bifurcation but will only be the trigger of the instability.

Narrow obstacle. – When the typical range of the obstacle potential is much smaller than the healing length, *i.e.*, when $\sigma \ll 1$, it is possible to approximate $U(x)$ by $U(x) = U_0 F(\sigma) \delta(x)$, where $F(\sigma)$ is the integral of $f(|x|/\sigma)$ over the whole real axis, and is simply given by $F(\sigma) = \sigma$ in the case of a square obstacle, which could be a well or a barrier depending on the sign of U_0 . One can then obtain an analytical expression for the supersonic separatrix by searching for the solutions of the Hamilton equations with energy $E_{cl,\delta} = \varepsilon(v_\infty) = 2U_0^2 F^2(\sigma) + v_\infty^2 + g(1) - G(1)$ associated to a δ -shaped obstacle.

From a classical point of view, the fictitious particle starts at $x = -\infty$ with density $n_\infty = 1$. It experiences a kick of energy when meeting the obstacle, going from W_{\min} to ε , and will oscillate between the two solutions of $W(n) = \varepsilon$ after this encounter. If $W_{\min} < \varepsilon < W_{\max}$, the particle is trapped and the density oscillates between the two solutions of $W(n) = \varepsilon$: This is the supersonic stationary regime. This type of solution is depicted in panel (c) of fig. 1. However if $\varepsilon < W_{\min}$ or $\varepsilon > W_{\max}$, the dynamics is no longer stationary and excitations are continuously generated as depicted in panel (b) of fig. 1.

The boundary between the nonstationary and the stationary regimes is by definition the supersonic separatrix, and corresponds to the last stationary solution. It is given by $\varepsilon(v_s) = W(n_{\max}(v_s))$ with n_{\max} such that $W'(n_{\max}) = 0$. This yields

$$\frac{1}{\sqrt{2}} \left[\frac{v_s^2}{2} \left(\sqrt{n_{\max}} - \frac{1}{\sqrt{n_{\max}}} \right)^2 + g(1)(n_{\max} - 1) + G(1) - G(n_{\max}) \right]^{\frac{1}{2}} = |U_0 F(\sigma)|. \quad (4)$$

An explicit solution of this equation can be derived for a cubic nonlinearity of the form $g(n) = n$ [18], while for a saturable nonlinearity of the form $g(n) = (1 + n_s)^2 n / [n_s(n + n_s)]$, characteristic of superfluids of light in a saturable media [21], it has to be solved numerically (see SM).

The upper panel of fig. 3 represents the supersonic separatrix with respect to the effective amplitude $U_0 F(\sigma)$ of the narrow obstacle. The green curve is obtained for a cubic nonlinearity, whereas the blue solid (dotted) lines are for a saturable nonlinearity, with saturation intensity $n_s = 0.1, 10$. Although the cubic nonlinearity is a limiting case of the saturable nonlinearity when $n_s \gg n$, large deviations are observable even for $n_s = 10$ which are of great importance for experiments with fluids of light. Moreover, it is important to emphasise that in the above-mentioned saturable systems, the fictitious potential $W(n)$ may be such that it has no local maximum depending on the value of n_s . With a saturable nonlinearity, when $v_\infty > \sqrt{2 + 2n_s}$, the potential W has only one minimum and diverges towards $+\infty$ for both $n \rightarrow 0$ and $n \rightarrow +\infty$ (see SM). The fictitious particle is then always trapped in this potential and all solutions for $v_\infty > \sqrt{2 + 2n_s}$ are

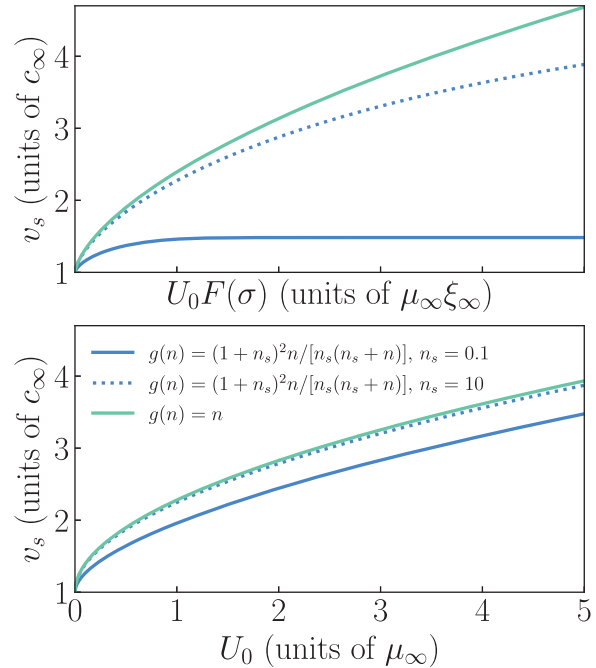


Fig. 3: The top (bottom) figure represents the supersonic separatrix for a repulsive narrow (wide) obstacle of amplitude $U_0 F(\sigma)$ (U_0). The two types of nonlinearity $g(n)$ considered here are indicated in the legend which applies to both panels.

stationary. This explains the plateau at large $U_0 F(\sigma)$ in the top panel of fig. 3 for the $n_s = 0.1$ case with a value $v_s = \sqrt{2.2} \simeq 1.48$. It is also interesting to note that eq. (4) predicts a symmetric supersonic separatrix as a function of U_0 . This symmetry between repulsive and attractive obstacle —not present in the case of the superfluid separatrix— is also a peculiarity of the δ -peak model, and will be broken as σ increases, or in other words when the velocity of the flow is large enough so that the associated de Broglie wavelength is small enough to resolve the details of the potential. This can be seen, for example, in fig. 1 where the symmetry is clearly broken and resonances appear in the attractive case for a square potential of width $\sigma = 1$ and a cubic nonlinearity.

Wide repulsive obstacle. – We now consider the obstacle dependence of the separatrix in the case of a wide obstacle $\sigma \gg 1$. In that case, the fictitious particle follows adiabatically the slow variations of the effective potential $W(n) - U(x)n$ and remains at its minimum as far as it exists. The situation is then similar to the one of a weak obstacle. The fluid flow is locally uniform but dressed by the obstacle according to eq. (2) with $A'' = 0$. It is now a matter of applying the criterion for the saddle-node bifurcation locally, namely looking for points where the local velocity is equal to the local speed of sound $c(x) = n(x)g'(n(x))$. This will first appear at the maximum of the scattering potential at $x = 0$. Using current conservation we obtain the implicit formula

$$g'(n_{0,c})n_{0,c}^3 = v_s^2, \quad (5)$$

where $n_{0,c}$ is the density at $x = 0$ at the transition point and can be computed from the saddle point equation $W'(n_{0,c}) - U_0 = 0$. Equation (5) is equivalent to $W''(n_{0,c}) = 0$ which is the second saddle point equation. It is important to note that this equation is the same for the supersonic and the subsonic separatrix but has two solutions respectively larger and smaller than c_∞ . As for the narrow barrier, this supersonic separatrix is represented in the bottom part of fig. 3 for an obstacle of typically large σ , and for the same kinds of nonlinearities. As a matter of fact, the effect of saturation of the nonlinearity is less pronounced for large obstacles than for narrow ones. Note that we do not display the attractive part since eq. (5) predicts that the critical velocity is always the sound velocity at this level of approximation.

Attractive obstacle of arbitrary width. – In the general case, the precise shape of the obstacle has an important influence as we will discuss in this section. In general, eq. (2) has to be solved numerically to obtain the equation of the separatrix, except for specific models such as piecewise constant obstacles [18]. However, as far as localised obstacles of the form discussed in this work are considered, the generic picture displayed in fig. 1 is valid. In particular, nonlinear resonances may exist and lead to a nontrivial structure of the stability diagram. In ref. [29] such resonances were considered in the case of a repulsive square well obstacle due to the Ramsauer-Townsend effect in arbitrary dimension. These solutions were put forward to be of great interest since they share an important property with superfluid solutions, and they do not experience friction with the obstacle although they are supersonic (see SM for a detailed analysis). However, they exist on specific curves (represented by the orange dotted curves in fig. 4) in the stability diagram and do not form a continuous family of solutions like the subsonic superfluid solutions. We then cannot find a real superfluid regime above the supersonic separatrix as these lines form a null measure set. In the following, we discuss in detail the case of an attractive potential and give explicit results for a square well potential. Results with a Gaussian potential are available in the SM. In particular we demonstrate that the lobe structure in the stability diagram of fig. 1 is indeed related to these resonances which continuously connect the superfluid solutions to superfluid-like solutions above the critical velocity along one-dimensional lines in parameter space (U_0, v_∞) .

From now on, we focus on the attractive case and exemplify our findings with a square well potential of amplitude U_0 and width σ , and complement the stability diagram with the knowledge of the transmission coefficient in the (U_0, v_∞) -plane. While in the linear case (*i.e.*, $g(n) = 0$ in eq. (1)) the reflection and transmission coefficients, as well as the position of the resonances, are well known [37], they cannot be defined easily in the nonlinear case as previously discussed. Nevertheless it is possible to give a proper definition of scattering amplitudes using the theory

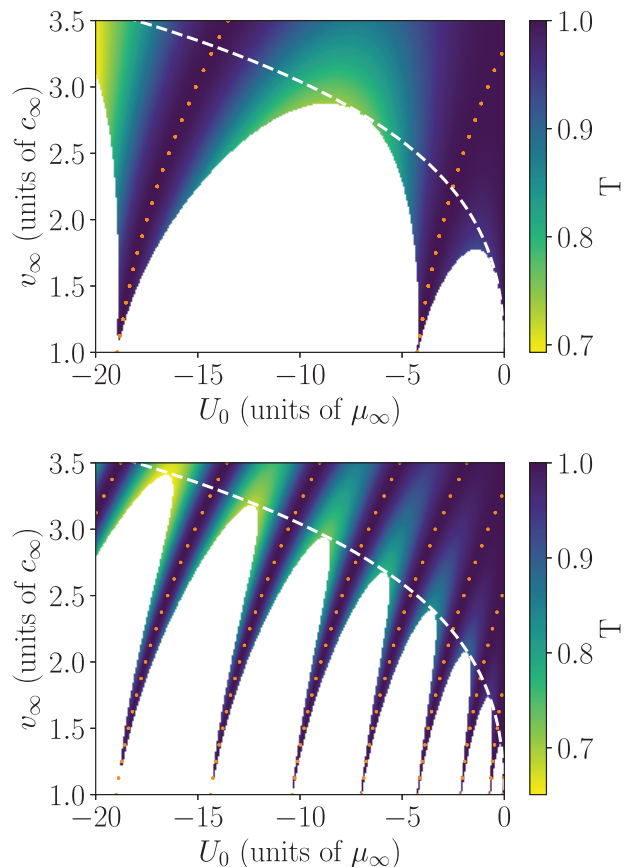


Fig. 4: Phase diagram (U_0, v_∞) (in the natural units of the superfluid) of a quantum fluid flowing across attractive square well potentials of respective width of $\sigma = 1$ (top) and $\sigma = 4$ (bottom), and for a cubic nonlinearity of the form $g(n) = n$. The transmission across the barrier is associated with the colour bar and is maximum along the orange dotted curves which determine the position of the resonances, whereas the white dashed line represents the envelope of the said resonances.

of adiabatic invariants [36,38] or a simpler but perturbative one in the weak backscattering limit [36,39]. As we are mostly interested in the position of the resonances, we will employ the latter definition which has been shown to produce results in good agreement with the exact adiabatic invariants approach [36] even far away from resonances. The transmission coefficient reads

$$T = \left(1 + \frac{\Delta E}{2(v_\infty^2 - 1)} \right)^{-1}. \quad (6)$$

ΔE is the energy difference of the fictitious particle between its final ($x = +\infty$) and initial ($x = -\infty$) states: $\Delta E = \mathcal{H}[A(x = +\infty), p(x = +\infty)] - \mathcal{H}[A(x = -\infty), p(x = -\infty)]$. For $x = -\infty$, the fictitious particle is at equilibrium with $A = 1$ and $p = 0$.

Numerical results are summarised in fig. 4. The colour scale shows the transmission coefficient of the fluid across the obstacle as a function of the injection velocity of the fluid and of the amplitude of the square well obstacle, for a given value of σ . The coloured zone is separated

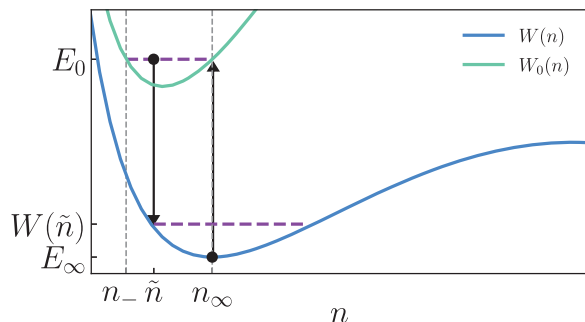


Fig. 5: Classical potentials seen by the fictitious particle in the case of an attractive square well obstacle. The lower curve is the potential $W(n)$ for $x < -\sigma/2$ and $x > \sigma/2$, while $W_0(n)$ is the one for $x \in [-\sigma/2, \sigma/2]$.

from white zones of undefined transmission (corresponding to the nonstationary regime) by the supersonic separatrix, clearly exhibiting resonances. In particular, the perfect transmission lines are shown to follow exactly the nontrivial structure of the stability diagram and are drawn as orange dotted curves, while the white dashed curve represents the envelope of the resonances. Both curves can be calculated analytically for a square well potential as suggested in [18] and explained below. In the following we provide explicit results for $g(n) = n$. Again, thinking in terms of a fictitious particle moving in a classical potential provides a simple picture of the underlying physics, and the mechanism behind the existence of resonances is illustrated in fig. 5.

We start by discussing the stability diagram. Before the excitation caused by the rectangular obstacle, the fictitious particle is at rest from $x = -\infty$ to $x = -\sigma/2$ with density n_∞ and energy $E_\infty = W(n_\infty)$ in the potential W . As it reaches the obstacle, it undergoes a kick of energy $\Delta E = E_0 - E_\infty$, going from (n_∞, E_∞) to (n_∞, E_0) in the new potential $W_0 = W + U_0 n$. The particle then oscillates in W_0 between n_∞ and n_- as it progresses in the obstacle, and returns to the potential W with density \tilde{n} for $x = +\sigma/2$. Several cases leading to different dynamics for the fluid are then possible depending on the values of U_0 , v_∞ and σ . In that context, we define \tilde{L} the distance between n_∞ and \tilde{n} performed in W_0 , and L_0 the distance of the round-trip between n_∞ and n_- , *i.e.*, the period of the oscillations of the fictitious particle in W_0 ,

$$\tilde{L} = \frac{1}{\sqrt{2}} \int_{\sqrt{\tilde{n}}}^{\sqrt{n_\infty}} \frac{dA}{\sqrt{E_0 - W_0(A)}}, \quad (7a)$$

$$L_0 = \sqrt{2} \int_{\sqrt{n_-}}^{\sqrt{n_\infty}} \frac{dA}{\sqrt{E_0 - W_0(A)}}. \quad (7b)$$

For stationary solutions to exist it is necessary that the energy of the fictitious particle when it exits the obstacle is lower than the maximum of $W(n)$ (the configuration of fig. 5). In this way, the particle is always confined. The envelope of the resonances (white dashed line in fig. 4), above

which stationary solutions exist no matter the value of σ , is obtained when the energy of the fictitious particle at the end of the obstacle corresponds exactly to the maximum of the fictitious potential. An analytical expression can be obtained for that envelope, separating the case where solutions always exist from the one where the existence of the said solutions depends on the value of σ , and can be found in eqs. (34) and (35) of [18]. It is interesting to note that, for a square well obstacle, U_0 and σ are uncorrelated quantities, and the amplitude of the resonances will not depend on σ , as shown by the white dashed line in fig. 4. For such an obstacle, the resonances will never disappear and their envelope will always be the same for any value of σ . Interestingly, numerical simulations showed that this is not the case for a Gaussian potential: The envelope of the resonances does depend on σ , and decreases as the width increases. These results are presented in the SM. One can also see in fig. 4 that the resonances multiply as σ increases. At some point, for an arbitrarily large value of σ , the resonances are so thin and numerous that they are not distinguishable from one another anymore, to the extent that the supersonic separatrix would be given by $v_s = 1$ in the limit $\sigma \gg 1$. Since the subsonic separatrix is also given by $v_c = 1$, the gap opened by the nonstationary regime slowly closes as the width of the obstacle increases.

Concerning the position of the resonances, the connection of the subsonic superfluid solution to curves of perfect transmission in the supersonic regime is performed at $v_\infty = c_\infty$. From our classical analysis, the two extrema of the potential $W(n)$ merge in a unique saddle point located at $n = n_\infty$. Oscillations are not possible anymore, and the only way for a stationary state to exist is when the excited fictitious particle exits W_0 with the same density it had when entering it, meaning $\tilde{L} = 0$. More generally, when the fictitious particle performs an arbitrary number of round-trips in the excited potential W_0 , so that its energy after exiting the obstacle is exactly the one it had before the excitation, a resonance forms between the width of the obstacle and the wavelength of the cnoidal wave of the oscillating particle, causing a perfect transmission, and linking the superfluid regime to the stationary nonsuperfluid one. The equation of these lines of perfect transmission (see the orange dotted curves in fig. 4) is then given by $\alpha L_0 = \sigma$, α being an integer, with L_0 given by eq. (7). Along these lines, the superfluid/stationary nonsuperfluid transition is continuous and the system is always stationary. Note that we have numerically checked the stability of this solution by doing time-dependent simulation of the NLS eq. (1). This was done in the spirit of ref. [29] where the obstacle was ramped adiabatically in strength and velocity.

Conclusion. – In this paper we have studied the supersonic separatrix between the nonstationary and the normal stationary regime of a generic quantum fluid flowing past a localised obstacle of arbitrary amplitude and

width, in the 1D mean-field regime. We have computed this critical velocity by deriving nonperturbative exact expressions in the limits of narrow and wide obstacle, and studying more thoroughly the peculiar case of the arbitrary attractive obstacle, which exhibits a nontrivial behaviour. For most parameters, a standing wave forms ahead of the obstacle, with a constant friction force and a partially transmitted wave. However we have shown that, along certain curves, due to resonant transport, supersonic solutions may share fundamental properties with their subsonic superfluid counterpart: They are symmetric solutions and, therefore, the quantum fluid is totally transmitted through the obstacle, without any friction.

All together, these results are important for the experimental studies of transport properties of quantum fluids described by a generalised NLS equation. They provide a clear map in parameter space of the different possible stationary regimes of flow for a quantum fluid, in order to guide experimental studies in the desired regime of nonlinear transport.

Finally, an extension of this work to higher dimensions would be desirable, notably in 2D, as experimental data are available for a saturable nonlinearity [21].

* * *

We thank P. VIGNOLO, M. BELLEC and C. MICHEL for inspiring discussions. This work has benefited from the financial support of Agence Nationale de la Recherche under Grants Nos. ANR-21-CE30-0008 STLight (Superfluid and Turbulent Light in Complex Media) and ANR-21-CE47-0009 Quantum-SOPHA (Quantum Simulators for One-Dimensional Systems with Photons and Atoms).

Data availability statement: The data that support the findings of this study are available upon reasonable request from the authors.

REFERENCES

- [1] LEGGETT A. J., *Rev. Mod. Phys.*, **71** (1999) S318.
- [2] KAPITZA P., *Nature*, **141** (1938) 74.
- [3] ALLEN J. F. and MISENER A. D., *Nature*, **141** (1938) 75.
- [4] OSHEROFF D. D., RICHARDSON R. C. and LEE D. M., *Phys. Rev. Lett.*, **141** (1972) 885.
- [5] RAMAN C. *et al.*, *Phys. Rev. Lett.*, **83** (1999) 2502.
- [6] AMO A. *et al.*, *Nat. Phys.*, **5** (2009) 805.
- [7] MICHEL C., BOUGHDAD O., ALBERT M., LARRÉ P.-É. and BELLEC M., *Nat. Commun.*, **9** (2018) 2108.
- [8] LANDAU L. D., *Phys. Rev.*, **60** (1941) 356.
- [9] LANDAU L. D., *J. Phys. USSR*, **5** (1941) 71.
- [10] PHILLIPS A. and MCCLINTOCK P. V. E., *Phys. Rev. Lett.*, **33** (1974) 1468.
- [11] GINZBURG V. L. and PITAEVSKII L. P., *Zh. Eksp. Teor. Fiz.*, **34** (1958) 1240.
- [12] GROSS E. P., *Il Nuovo Cimento*, **20** (1961) 354.
- [13] PITAEVSKII L. P., *J. Phys. USSR*, **13** (1961) 451.
- [14] FRISCH T., POMEAU Y. and RICA S., *Phys. Rev. Lett.*, **69** (1992) 1644.
- [15] HUYNH J., ALBERT M. and LARRÉ P.-É., *Phys. Rev. A*, **105** (2022) 023305.
- [16] PITAEVSKII L. P. and STRINGARI S., *Bose-Einstein Condensation and Superfluidity* (Oxford University Press, Oxford) 2016.
- [17] CARUSOTTO I. and CIUTI C., *Rev. Mod. Phys.*, **85** (2013) 299.
- [18] LEBOEUF P. and PAVLOFF N., *Phys. Rev. A*, **64** (2001) 033602.
- [19] ENGELS P. and ATHERTON C., *Phys. Rev. Lett.*, **99** (2007) 160405.
- [20] DRIES D., POLLACK S. E., HITCHCOCK J. M. and HULET R. G., *Phys. Rev. A*, **82** (2010) 033603.
- [21] ELOY A., BOUGHDAD O., ALBERT M., LARRÉ P.-É., MORTESSAGNE F., BELLEC M. and MICHEL C., *EPL*, **134** (2021) 26001.
- [22] NAZARENKO S., *Wave Turbulence, Lect. Notes Phys.*, Vol. **825** (Springer Science & Business Media) 2011.
- [23] BARENGHI C. F., SKRBEC L. and SREENIVASAN K. R., *Proc. Natl. Acad. Sci. U.S.A.*, **111** (2014) 4647.
- [24] LESZCZYŹYŹN A. M., EL G. A., GLADUSH YU. G. and KAMCHATNOV A. M., *Phys. Rev. A*, **79** (2009) 063608.
- [25] KAMCHATNOV A. M. and PAVLOFF N., *Phys. Rev. A*, **85** (2012) 033603.
- [26] PAUL T., RICHTER K. and SCHLAGHECK P., *Phys. Rev. Lett.*, **94** (2005) 020404.
- [27] RAPEDIUS K., WITTHAUT D. and KORSCH H. J., *Phys. Rev. A*, **73** (2006) 033608.
- [28] RAPEDIUS K. and KORSCH H. J., *Phys. Rev. A*, **77** (2008) 063610.
- [29] PARIS-MANDOKI A., SHEARRING J., MANCARELLA F., FROMHOLD T. M., TROMBETTONI A. and KRÜGER P., *Sci. Rep.*, **7** (2015) 9070.
- [30] FONTAINE Q., BIENAIMÉ T., PIGEON S., GIACOBINO E., BRAMATI A. and GLORIEUX Q., *Phys. Rev. Lett.*, **121** (2018) 183604.
- [31] VOCKE D., WILSON K., MARINO F., CARUSOTTO I., WRIGHT E. M., RODGER T., ANDERSON B. P., ÖHBERG P. and FACCIO D., *Phys. Rev. A*, **94** (2016) 013849.
- [32] LEBOEUF P. and MOULIERAS S., *Phys. Rev. Lett.*, **105** (2010) 163904.
- [33] LARRÉ P.-É. and CARUSOTTO I., *Phys. Rev. A*, **92** (2015) 043802.
- [34] ŠANTIĆ N., FUSARO A., SALEM S., GARNIER J., PICOZZI A. and KAISER R., *Phys. Rev. Lett.*, **120** (2018) 055301.
- [35] LAMB H., *Hydrodynamics* (Cambridge University Press, Cambridge) 1997.
- [36] PAUL T., HARTUNG M., RICHTER K. and SCHLAGHECK P., *Phys. Rev. A*, **76** (2007) 063605.
- [37] GRIFFITHS D. J. and SCHROETER D. F., *Introduction to Quantum Mechanics* (Cambridge University Press, Cambridge) 2018.
- [38] LANDAU L. D. and LIFSHITZ E., *Mechanics*, third edition, Vol. **1** (*Course of Theoretical Physics*) (Butterworth-Heinemann) 1976.
- [39] PAUL T., ALBERT M., SCHLAGHECK P., LEBOEUF P. and PAVLOFF N., *Phys. Rev. A*, **80** (2009) 033615.